NASA TECHNICAL MEMORANDUM

WIND-TUNNEL INVESTIGATION
OF TECHNIQUES FOR REDUCING COWL DRAG
OF AN AXISYMMETRIC EXTERNAL-COMPRESSION
INLET AT MACH 2.49

by James E. Calogeras and Edward T. Meleason

Lewis Research Center

Cleveland, Ohio

NATIONAL AERONAUTICS AND SPACE ADMINISTRATION • WASHINGTON, D. C. • MARCH 1968

WIND-TUNNEL INVESTIGATION OF TECHNIQUES FOR REDUCING COWL

DRAG OF AN AXISYMMETRIC EXTERNAL-COMPRESSION

INLET AT MACH 2.49

By James E. Calogeras and Edward T. Meleason

Lewis Research Center
Cleveland, Ohio

NATIONAL AERONAUTICS AND SPACE ADMINISTRATION

WIND-TUNNEL INVESTIGATION OF TECHNIQUES FOR REDUCING COWL DRAG OF AN AXISYMMETRIC EXTERNAL-COMPRESSION INLET AT MACH 2.49

by James E. Calogeras and Edward T. Meleason

Lewis Research Center

SUMMARY

A wind-tunnel investigation was made at Mach 2.49 to determine the effectiveness of two techniques for cowl-drag reduction on an axisymmetric external-compression inlet. The first method involved reducing the external cowl-lip angle from 25° to values of 15° and 6°. Use of the flatter cowls deliberately violated the criterion for internal cowl-lip shock attachment to affect a tradeoff between cowl pressure drag and induced additive drag. Results showed an increase in external drag over that associated with the 25° cowl, and inlet performance was significantly reduced with use of the flatter cowls. The second method used a low-external-angle visor with the 25° cowl. An air gap existed between the cowl and the visor base to aid in starting the inlet, and several gap sizes were investigated. With the smallest air gap tested, external drag was reduced by 54 percent with only a small loss in performance. With a larger air gap sized to permit self-start at Mach 2.5, external drag was reduced by 35 percent; this reduction, however, was accompanied by some loss in overall inlet performance associated with flow expansion into the visor gap.

INTRODUCTION

A major problem associated with the use of high-performance external-compression inlets for supersonic cruise applications is the high cowl-drag characteristic of this type inlet (e.g., ref. 1, p. 627). Several investigations aimed at reducing this drag have already been made. An analysis based on momentum and continuity considerations was made in reference 2, in which pressure recovery was traded for drag reduction by limiting the amount of external compression. Internal contraction was introduced into a two-dimensional inlet in reference 3 to effectively reduce cowl drag without degrading inlet performance. Unless internal contraction is limited, however, this type inlet has

inherent starting problems. A visor-like cowl extension with a low external angle and an internal surface parallel to free stream at zero-degree angle of attack was also used in reference 3 to reduce the effective cowl angle. Results showed a significant reduction in cowl drag with only a small penalty in performance at design conditions. A partial shield similar to the visor of reference 3 was investigated on an axisymmetric inlet in reference 4. The purpose of the shield, however, was to reduce the adverse effects of angle of attack on inlet performance rather than to reduce cowl drag.

The present investigation was conducted in the Lewis 10- by 10-Foot Supersonic Wind Tunnel to study the effects of cowl-drag reduction techniques on the performance of an axisymmetric external-compression inlet. Data were obtained at the inlet design Mach number of 2.49 for angles of attack from 0° to 5°. Two methods of reducing cowl drag were studied. The first method was to lower the cowl angle of a high-performance inlet configuration below the angle required for internal cowl-lip shock attachment. Internal centerbodies for the flatter cowls were designed so that internal contraction (and, hence, an inlet start problem) was avoided. Two configurations with reduced cowl angles were tested, and results are presented in this report.

The second method which was investigated included the use of an internally cylindrical, low-external-angle visor mounted coaxially with the high-performance inlet configuration. By translating the visor, an air gap between the visor base and the external cowl surface was sized to allow self-start at Mach 2.49. Since a more sophisticated visor design might incorporate aerodynamically actuated flaps into the visor base to allow self-start capability at reduced gap sizes, data were obtained at several air-gap settings. In addition, two visor configurations differing in base geometries were investigated, and results of both are presented herein.

SYMBOLS

A_G minimum area between visor and external cowl surface, in.^{2} (cm^2)

A_i projected cowl-lip area, 162.2 in.^{2} (1046.45 cm^2)

A_s minimum area between basic visor and centerbody, in.^{2} (cm^2)

A_s' minimum area between modified visor and centerbody, in.^{2} (cm^2)

A_t throat area, 69.4 in.^{2} (176.28 cm^2)

C_D external drag coefficient based on projected cowl-lip area

C_{D_A} additive drag coefficient based on projected cowl-lip area

C_{D_P} pressure-drag coefficient based on projected cowl-lip area

L visor extension, in. (cm)

L_D diffuser length, 28.45 in. (72.26 cm)

M   Mach number

m   mass flow, lb/sec (kg/sec)

m_{sp} spillage mass flow, lb/sec (kg/sec)

P   total pressure, lb/ft^2 abs (N/m^2 abs)

p   static pressure, lb/ft^2 abs (N/m^2 abs)

r_i cowl-lip radius, 7.185 in. (18.25 cm)

x   axial distance, in. (cm)

y   radial distance, in. (cm)

α angle of attack, deg

λ flow angle, deg

Subscripts:

crit   critical inlet operation

f   focal point

max   maximum

min   minimum

s   spike surface

x   conditions at x-distance

0   conditions in free stream

2   conditions at diffuser exit (compressor face)

(–)   area-weighted average

APPARATUS AND PROCEDURE

The basic high-performance external-compression inlet used to evaluate the various drag-reduction techniques is shown in figure 1. This inlet had an external cowl-lip angle of 25° (hereinafter referred to as the 25° inlet) and was designed for a free-stream Mach number of 2.5. The spike was designed for 99-percent total-pressure recovery through the initial shock followed by isentropic focused compression to an average Mach number of 1.389 at the throat. Compression was limited by the shock-structure criterion presented in reference 5 with the assumption of an effective compression of 1° due to boundary-layer growth. Spike coordinates were obtained from results presented in

table I of reference 5 adjusted for continuity considerations. With an assumed 5-percent total-pressure loss in subsonic diffusion, the maximum theoretical diffuser exit recovery was 0.90.

The three inlets used in the cowl-angle test are shown schematically in figure 2. Flow conditions at the focal point required an internal cowl-lip angle of 20° or greater for internal lip shock attachment. The internal cowl-lip angle of the 25° inlet provided a 2° margin for shock attachment; however, internal cowl-lip angles of the 15° and 6° inlets were, respectively, 8° and 17° beyond this limit. Centerbody flush slots were sized to bleed from 5 percent of the captured mass flow for the 25° inlet to about 10 percent for the 6° inlet during critical operation.

It became evident during the cowl-angle test that the isentropic compression waves were not focusing properly. This was attributed to improper spike contouring, and a computer program, written at Lewis and based on the method of characteristics, was used to recontour the spike surface for subsequent testing. The characteristics solution of the revised spike surface is presented in figure 3. Enough expansion was introduced on the centerbody to provide a uniform Mach number at the cowl-lip station, which, in turn, relieved compression along the initial portion of the internal cowl surface during supercritical inlet operation. Spike compression was reduced from 38° to $36\frac{1}{2}^{\circ}$ to allow a 5° margin between the turning angle at the cowl lip with the 25° inlet and the theoretical internal shock detachment angle. Surface Mach-number and flow-angle distributions are also shown in figure 3, together with the original spike distributions.

Altogether, four distinct versions of the 25° inlet were tested. These configurations are shown schematically in figure 4. Configurations A and B differ only in that the amount of external turning along the spike was reduced by 1.5° for configuration B in an attempt to improve flow conditions at the cowl lip. For both configurations, the forward edge of the bleed slot was located at the terminal-shock impingement point for critical inlet operation. The recontoured spike was used in configuration C, and perforated centerbody bleed was located just forward of the point where the oblique shock impinges during supercritical inlet operation. For configuration D, perforated bleed was located just aft of the oblique-shock impingement.

Flow-area variations in the subsonic diffuser are shown in figure 5 for the three inlets used in the cowl-angle test. The equivalent conical diffusion was 9.4°. Spike revisions had little effect on internal area variations and, hence, are not shown.

Visor configurations tested with the 25° inlet are presented schematically in figure 6. The visors were manually translatable and were designed to capture the full inlet mass flow. During the test program, the basic visor was modified as shown to allow inlet start at smaller visor extensions. Minimum area variations with visor extension are shown in figure 7 for both visored inlet configurations. It is apparent that at large extension ratios, the minimum area lies between the visor and centerbody for both configurations. At extension ratios below 0.474 with the modified visor, however, the minimum

4

area becomes a combination of inlet throat area and gap area between the visor and external cowl.

Inlet mass flow was regulated with a sonic plug and was computed from the sonic area and an average static pressure at a fixed area just upstream of the plug. An area-weighted average of 36 total pressure measurements at the diffuser exit was used to determine pressure recovery and distortion. Cowl-pressure-drag coefficients were computed from six area-weighted static-pressure measurements along the external cowl surface. Similarly, five area-weighted static pressures along the external visor surface and six along the visor base were used to compute visor pressure drag.

RESULTS AND DISCUSSION

Variable-Cowl-Angle Test Results

Performance of the various external-compression inlets used in the cowl-angle test is presented in figure 8. Large losses in critical total-pressure recovery and mass flow ratio for the 15° and the 6° inlets were caused by detached-cowl-lip shocks. Critical distortion, however, decreased as the cowl angle was reduced. The large stable mass flow range demonstrated by the 6° inlet probably resulted from the extent of cowl shock detachment associated with that inlet. Schlieren photographs showing the three inlets during supercritical operation at Mach 2.49 and zero-degree angle of attack are presented in figure 9. A close inspection of the cowl-lip region in figure 9(a) reveals a slight shock detachment, which was probably caused by a combination of poor focusing of the isentropic compression waves and proximity to the detachment limit. Approximately 3 percent of the design capture mass flow was spilled through this detached shock. Figures 9(b) and (c) show the forward progression of the detached shock as the cowl angle was lowered. Flow spillage through the detached shocks amounted to 10 percent of the design capture mass flow for the 15° inlet and 23 percent for the 6° inlet. Spillages are based on an estimated bleed flow of between 2 and 3 percent for the three inlets during supercritical operation. Failure to achieve design bleed flow rates of from 5 to 10 percent may have been a factor in the generally low performance levels obtained with these configurations.

External drag coefficients based on projected cowl-lip area are presented in figure 10 for the three inlets. Additive drag coefficients were calculated by methods presented in reference 6. For these calculations, the actual cone-tipped isentropic compression spike was approximated by a 30° half-angle cone, and spillage was assumed to be through the mechanism of a detached shock. Because of hardware limitations, all external cowl surfaces were faired to the same maximum nacelle diameter, which was

5

dictated by the 25° cowl. External coordinates for the three cowls are presented in table I. Since it would have been possible to use smaller nacelles (and, hence, smaller projected areas) with the flatter cowls, the effect of lowering cowl-lip angle is not entirely represented by the computed cowl pressure drags. In any case, the possibility of further reduction of cowl pressure drag becomes academic when performance degradation, as previously shown in figure 8, is considered together with increased external drags incurred by deliberately detaching cowl-lip shocks. As shown in figure 10, additive drag penalties outweighed pressure-drag reductions for the flatter cowls.

Spike and Bleed Optimization for 25° Inlet

The effect of the various spike and bleed modifications on performance of the 25° inlet is shown in figure 11. Configuration A, the original inlet design, had a peak total-pressure recovery of only 0.848. When the amount of external turning was reduced by 1.5° (configuration B), peak recovery increased to 0.870 and critical distortion decreased from 0.163 to 0.106; however, no subcritical stability was achieved. When the spike was recontoured and flush slot bleed replaced by perforated bleed (configuration C), inlet performance improved considerably with peak recovery increasing to 0.896. Finally, when the perforated bleed location was moved aft (configuration D), peak recovery increased to 0.927, and a stable subcritical mass flow range of about 3 percent was achieved because of increased bleed.

Schlieren photographs comparing the focusing characteristics of the recontoured spike with those of the original design are shown in figure 12. Focusing was clearly improved by the revision. A schlieren photograph of configuration D during supercritical inlet operation is shown in figure 13. Comparison of this figure with figure 9(a) illustrates the improvement in flow conditions at the cowl lip, although a slight shock detachment at the lip remained.

The effect of angle of attack on critical inlet performance is presented in figure 14. Configurations C and D provided the best performance over the angle-of-attack range investigated.

Cowl Visor Test Results

The effect of the basic visor on performance of configuration C is presented in figure 15 for various ratios of visor extension to cowl-lip radius (hereinafter called visor extension ratio, L/r_i). The best visored-inlet performance occurred at the smallest extension ratio tested. At this extension ratio ($L/r_i = 0.4036$), the peak inlet pressure

recovery of 0.896 was not affected by the visor, but the mass flow ratio at peak recovery was reduced from 0.937 to 0.887. Reduction in supercritical mass flow ratio was less severe, from 0.950 to 0.917. At visor extension ratios of 0.4913 and 0.5344, peak recovery was reduced to 0.855 at a mass flow ratio of about 0.825. A schlieren photograph of the visored inlet during supercritical operation at $L/r_i = 0.4913$ is shown in figure 16. Flow spillage, induced by expansion around the visor trailing edge, is shown emanating from the air gap between the visor and the cowl.

The performance of the same visored-inlet configuration is presented in figure 17 for various angles of attack. Performance of configuration C without the visor is also presented for comparison. Less sensitivity to effects of angle of attack is evident with the visored inlet so that as angle of attack increases, performance of the visored configuration more closely approaches that of the clean inlet.

Visor extension ratios required to allow inlet self-start at various free-stream Mach numbers are presented in figure 18 for the basic and modified visors. Since the visors were not remotely translatable, these results were obtained by varying test-section Mach number until the inlet started. Geometric throat areas at start for the basic and modified visor inlets (obtained from figs. 7 and 18) were, respectively, 106 and 102 percent of the theoretical throat area required for inlet start with normal shock recovery at free-stream Mach number. These percentages remained constant over the range of Mach numbers tested.

Inlet performance with the modified visor is presented in figure 19 for various visor extension ratios. Inlet configurations C and D were used with the modified visor. Regardless of the extension ratio investigated, neither inlet configuration used with the modified visor equaled the performance yielded by configuration C with the basic visor at an extension ratio of 0.4036 (fig. 15).

Visor-induced-spillage mass flow ratios are presented in figure 20 for various extension ratios. Spillages were calculated as the difference between supercritical mass flow ratios of the clean inlet and those of the visored inlet. As the basic visor was extended from $L/r_i = 0.4036$ to $L/r_i = 0.4913$ (Mach 2.5 self-start position), spillage increased from 2.8 to 8.6 percent of the design capture mass flow. Translating the modified visor had no effect on the amount of flow spilled through the visor gap, approximately 10 percent.

The effect of the basic visor on external drag is presented in figure 21 for various extension ratios. Additive drag due to the slight cowl-lip detached wave was neglected since the exact amount of spillage through this mechanism could not be determined. The drag contribution of the visor-induced spillage was calculated by using spillage mass flows from figure 20 and assuming that this flow underwent an expansion from free-stream static pressure to visor base pressure. The resulting additive drag force was negative. Considerable external drag reductions were obtained with both the basic and

the modified visors. At the smallest basic-visor extension tested, drag was reduced by 54 percent. With the basic visor positioned for self-start at Mach 2.5, external drag was reduced by 35 percent. Drag reduction for the modified-visor - inlet combination is not shown but was nearly constant at 38 percent for all extensions tested.

Typical pressure distributions on the visor and external cowl surfaces are presented in figure 22 for both the basic and the modified visor. At a basic-visor extension ratio of 0.4036, base pressures were significantly higher than for any other extension tested with either the basic or the modified visor. Because of this higher base pressure, this particular test condition exhibited the smallest induced flow spillage, the best overall performance, and the least external drag. A visor design which would keep pressure in the air gap at free-stream static pressure would probably further reduce drag without penalizing inlet performance. Such a design might incorporate aerodynamically actuated flaps into the visor base to allow self-start capability at reduced gap sizes. For the modified visor, base pressure was low and did not change appreciably with extension ratio. This resulted in approximately constant levels of inlet performance and visor-induced spillage.

SUMMARY OF RESULTS

An investigation was made to determine the effect on inlet performance of two methods of reducing the cowl drag of a high-performance external-compression inlet. The first method involved reducing the external cowl-lip angle from 25° to values of 15° and 6°. Use of the flatter cowls deliberately violated the criterion for internal cowl-lip shock attachment to affect a tradeoff between cowl pressure drag and induced additive drag. The second method used a low-external-angle visor with the 25° cowl. An air gap existed between the cowl and visor base to aid in starting the inlet. The size of the air gap was varied by extending the visor; data were obtained for several visor extensions including the one allowing inlet self-start at Mach 2.5. The visor was modified during the program to allow self-start at a smaller visor-to-cowl extension. The investigation was made at Mach 2.49 for angles of attack from 0° to 5°. The following results were obtained:

1. Flattening the cowl resulted in progressively worse performance. Furthermore, additive drag penalties incurred by deliberately detaching cowl-lip shocks exceeded pressure-drag reductions.

2. At the smallest basic-visor extension investigated, external drag was reduced by 54 percent with only a small loss in performance. Visor base pressures were much higher at this extension than at the larger visor extensions.

3. Use of the basic visor reduced external drag by 35 percent at the visor extension

8

required for self-start at Mach 2.5. This reduction, however, occurred at the expanse of a significant loss of inlet performance. At the peak pressure recovery point, recovery was reduced from 0.896 to 0.855 and mass flow ratio from 0.937 to 0.825.

4. External drag reduction incurred through use of the modified visor was nearly constant at 38 percent for all visor extensions tested. Performance penalties with this configuration were comparable to those incurred with the basic visor at positions which also permitted self-start.

Lewis Research Center,
    National Aeronautics and Space Administration,
        Cleveland, Ohio, November 15, 1967,
            720-03-01-62-22.

REFERENCES

1. Evvard, J. C.: Diffusers and Nozzles - Diffusers and Air Intakes. Aerodynamic Components of Aircraft at High Speeds. Vol. VII of High Speed Aerodynamics and Jet Propulsion. A. F. Donovan and H. R. Lawrence, eds., Princeton Univ. Press, 1957, pp. 586-638.

2. Meyer, Rudolph C.: Flow-Turning Losses Associated with Zero-Drag External-Compression Supersonic Inlets. NACA TN 4096, 1957.

3. Gertsma, Lawrence W.: Effect on Inlet Performance of a Cowl Visor and an Internal-Contraction Cowl for Drag Reduction at Mach Numbers 3.07 and 1.89. NASA Memo 3-18-59E, 1959.

4. Beheim, Milton A.; and Piercy, Thomas G.: Preliminary Investigation of Shield to Improve Angle-of-Attack Performance of Nacelle-Type Inlet. NACA RM E57G25a, 1957.

5. Connors, James F.; and Meyer, Rudolph C.: Design Criteria for Axisymmetric and Two-Dimensional Supersonic Inlets and Exits. NACA TN 3589, 1956.

6. Sibulkin, Merwin: Theoretical and Experimental Investigation of Additive Drag. NACA RM E51B13, 1951.

TABLE I. - EXTERNAL COWL SURFACE

COORDINATES

[Cowl-lip radius, r_i, 7.185 in. (18.25 cm).]
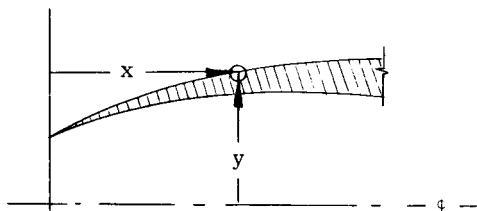
Axial distance ratio, x/r_i	Radial distance ratio, y/r_i	Axial distance ratio, x/r_i	Radial distance ratio, y/r_i
25° Inlet		15° Inlet	
0	[a]1.000	0	[a]1.000
.274	[a]1.130	.727	[a]1.195
.309	1.139	.796	1.211
.379	1.161	.866	1.228
.448	1.180	.935	1.242
.518	1.198	1.005	1.255
.587	1.214	1.144	1.277
.657	1.228	1.283	1.294
.727	1.240	1.422	1.395
.796	1.250	1.562	1.313
.866	1.260	1.701	1.317
.935	1.267	1.840	1.319
1.005	1.273	1.979	[a]1.322
1.144	1.286	2.647	[a]1.322
1.214	1.291		
1.283	1.296	6° Inlet	
1.562	1.314		
1.840	[a]1.322	0	[a]1.000
2.647	[a]1.322	2.647	[a]1.322

[a]Dimensions represent straight taper.
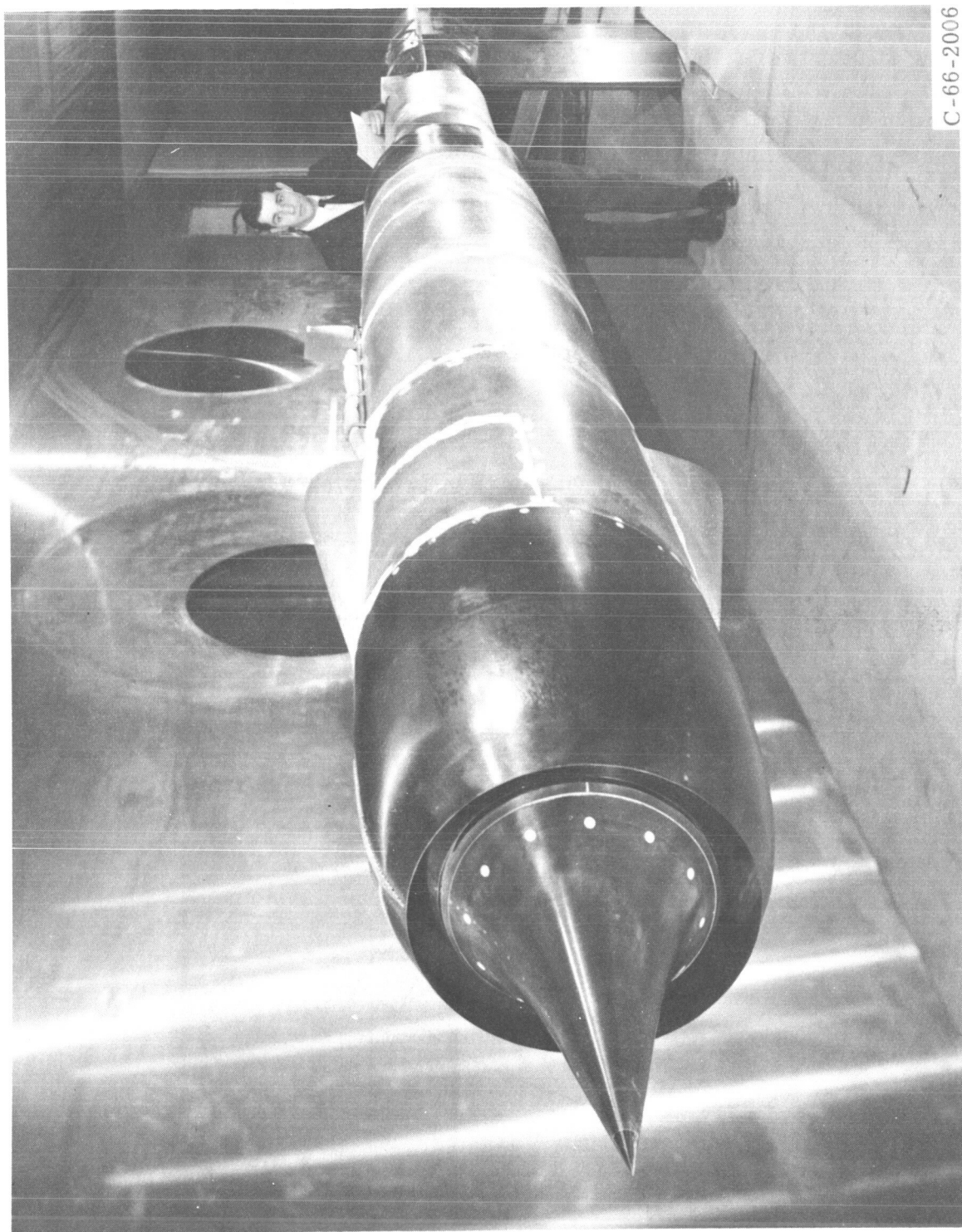
Figure 1. - External-compression inlet with 25° external cowl-lip angle.
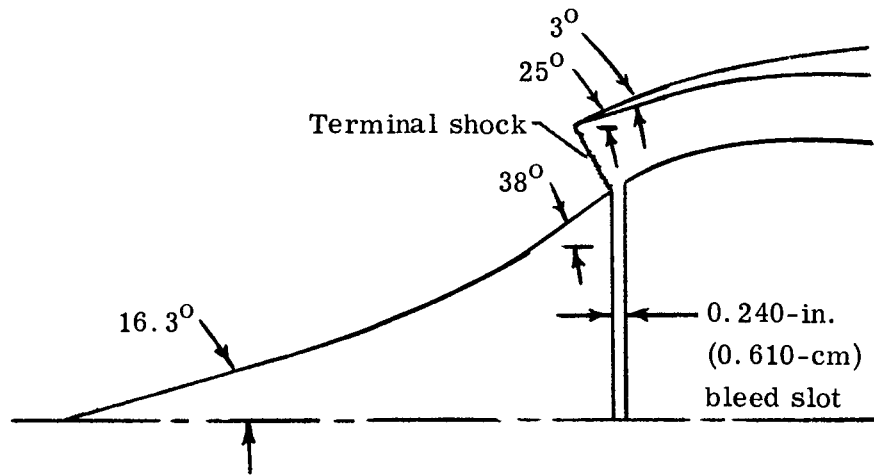
(a) 25° External cowl.
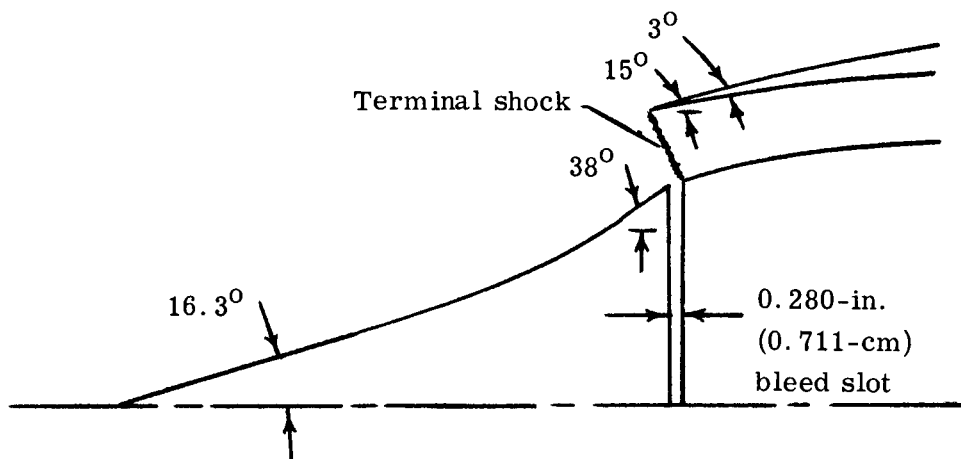
(b) 15° External cowl.
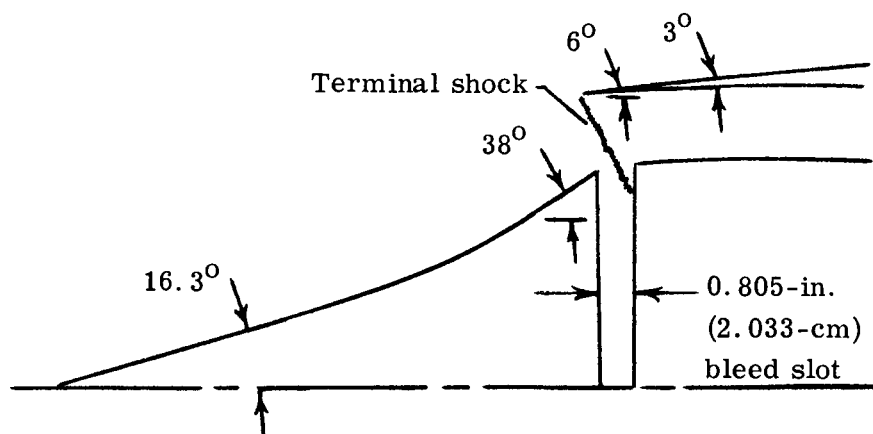
(c) 6° External cowl.

Figure 2. - Cowl and bleed configurations used in cowl-angle test.
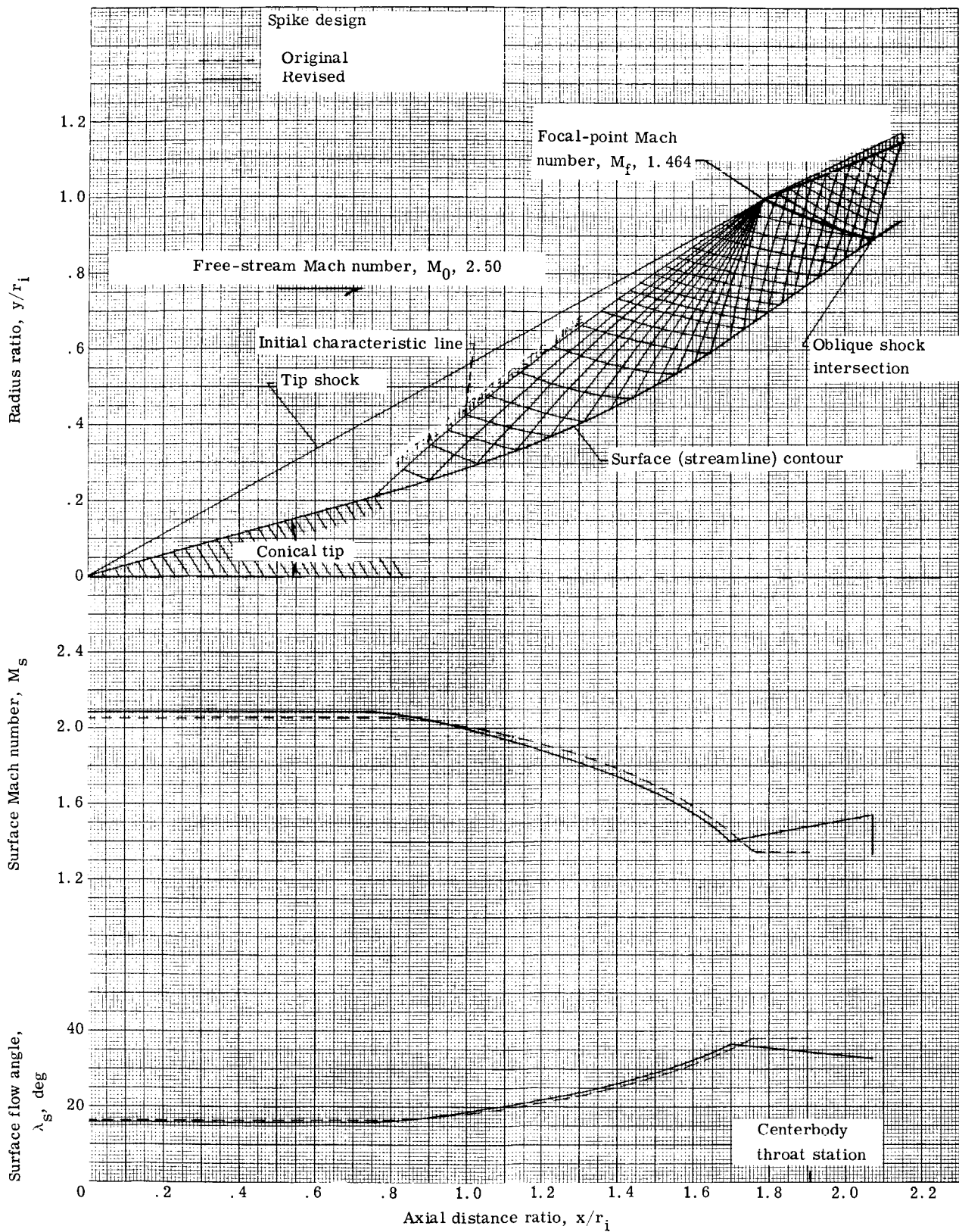
Figure 3. - Axisymmetric characteristics solution for revised isentropic spike configuration.
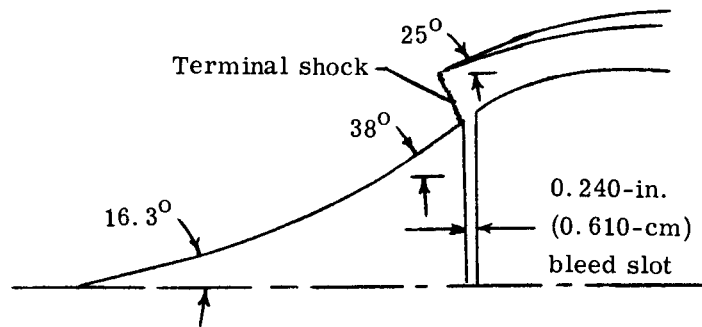
(a) Configuration A.
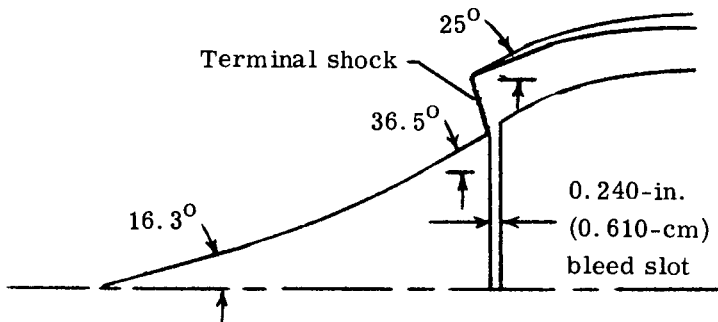
(b) Configuration B.
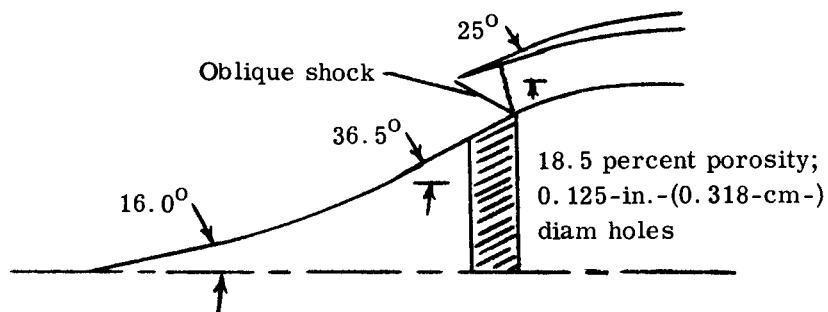
(c) Configuration C.
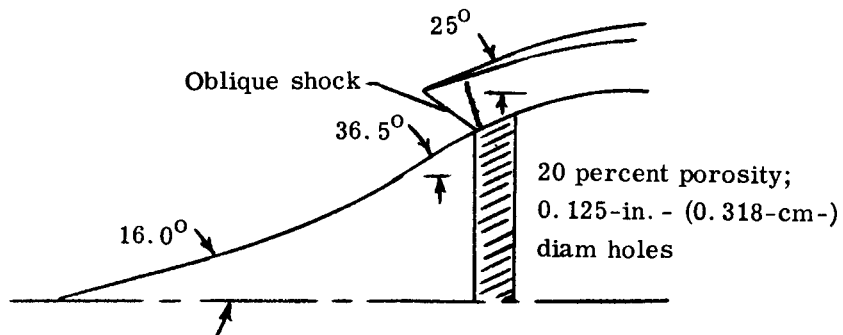
(d) Configuration D.

Figure 4. - Spike and bleed modifications.
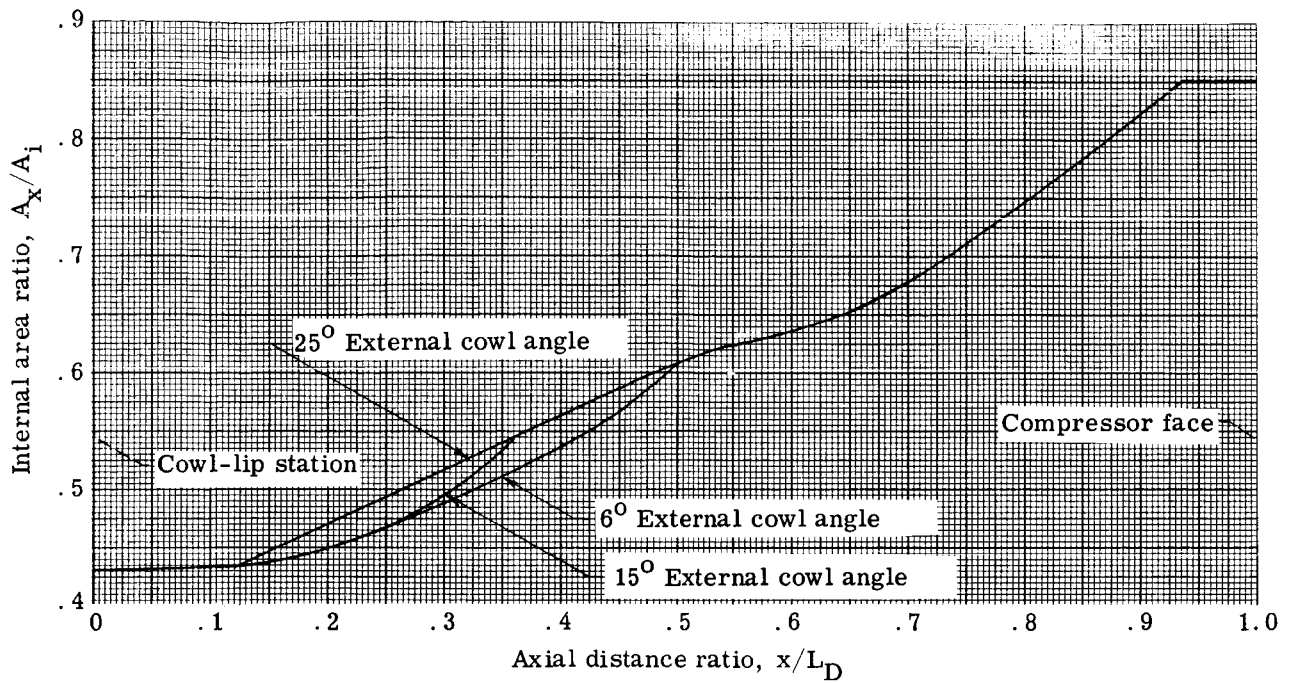
Figure 5. – Variation of diffuser internal area ratio for various cowl configurations. Diffuser length, 28.45 inches (72.26 cm); projected cowl-lip area, 162.2 square inches (1046.45 cm^2).
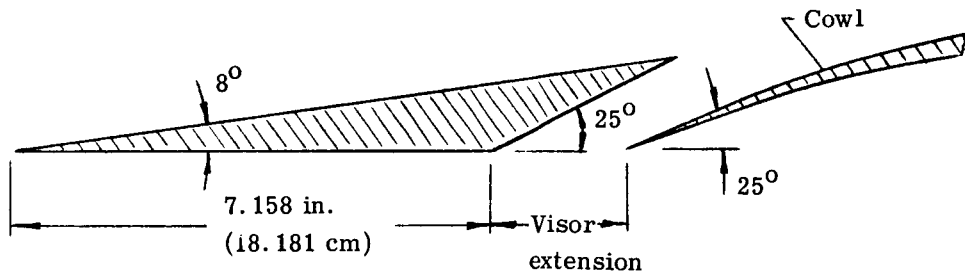
(a) Basic visor configuration.
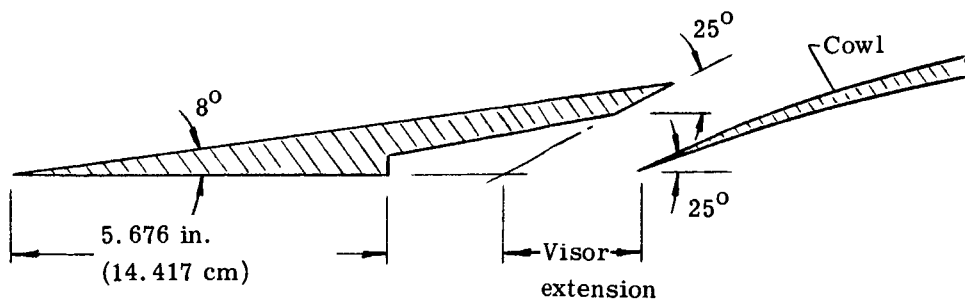
(b) Modified visor configuration.

Figure 6. – Schematic drawings of cowl visors.
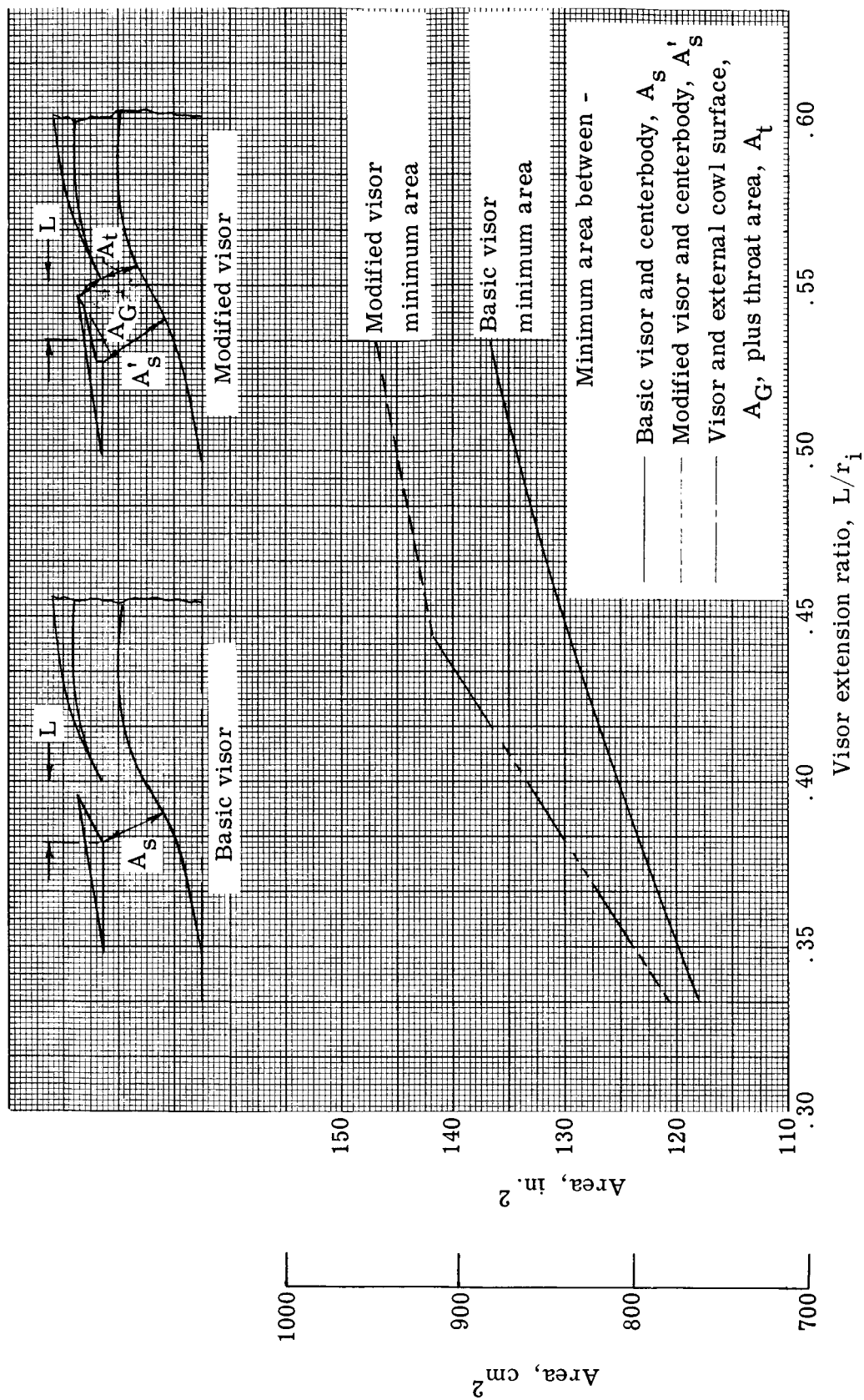
Figure 7. - Variation of minimum geometric area with visor position.
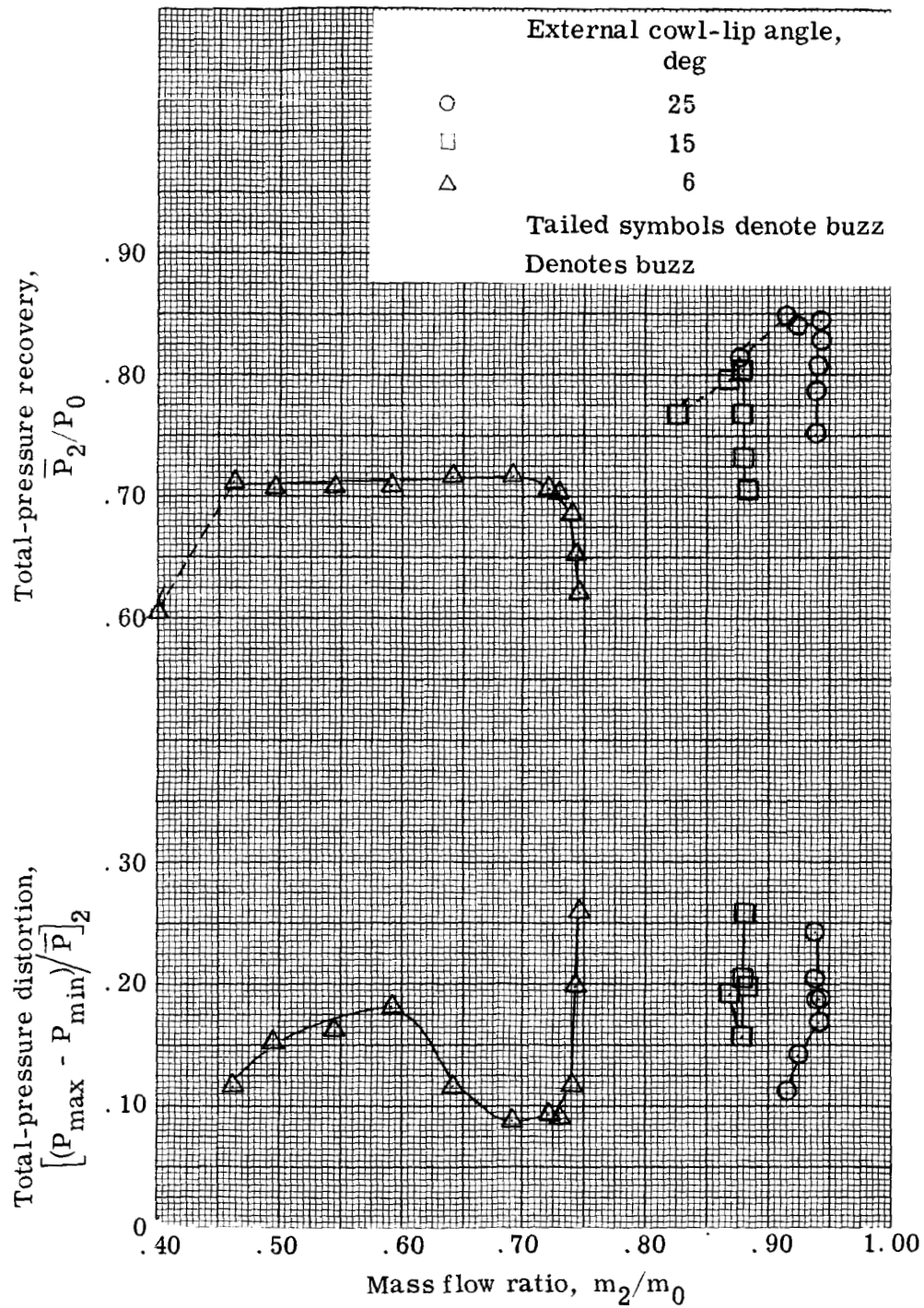
Figure 8. - Effect of cowl angle on inlet performance at Mach 2.49; angle of attack, 0°.
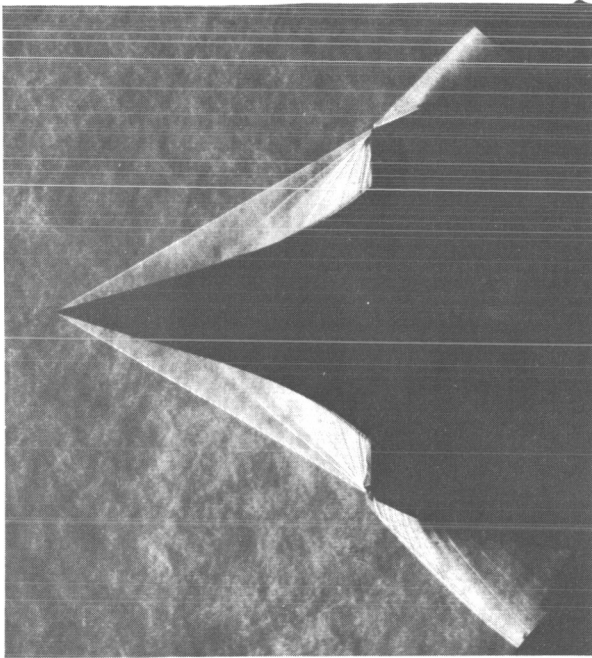
(a) 25° External cowl-lip angle inlet.
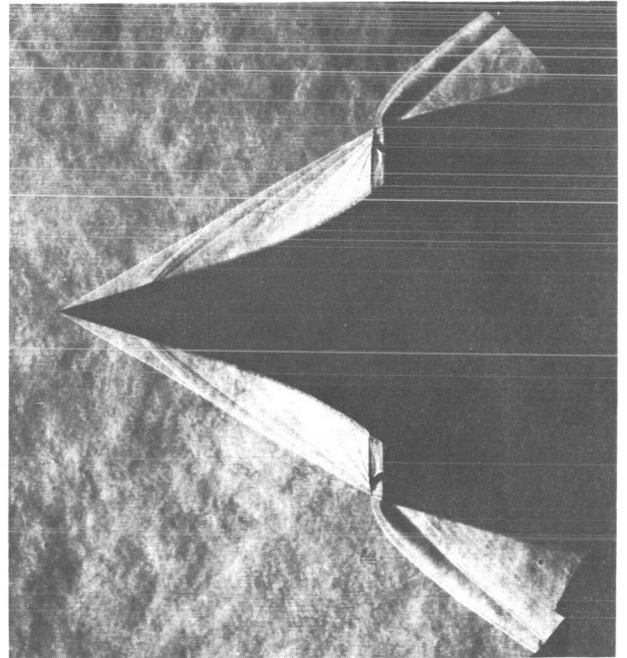
(b) 15° External cowl-lip angle inlet.
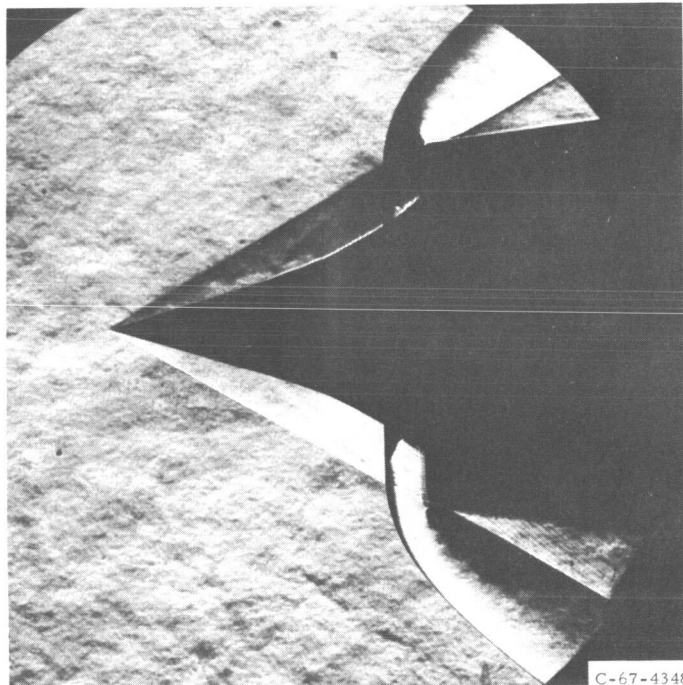
(c) 6° External cowl-lip angle inlet.

Figure 9. - Typical schlieren photographs showing supercritical operation of inlets used in cowl-angle test with original spike at free-stream Mach number of 2.49 and angle of attack of 0°.

18
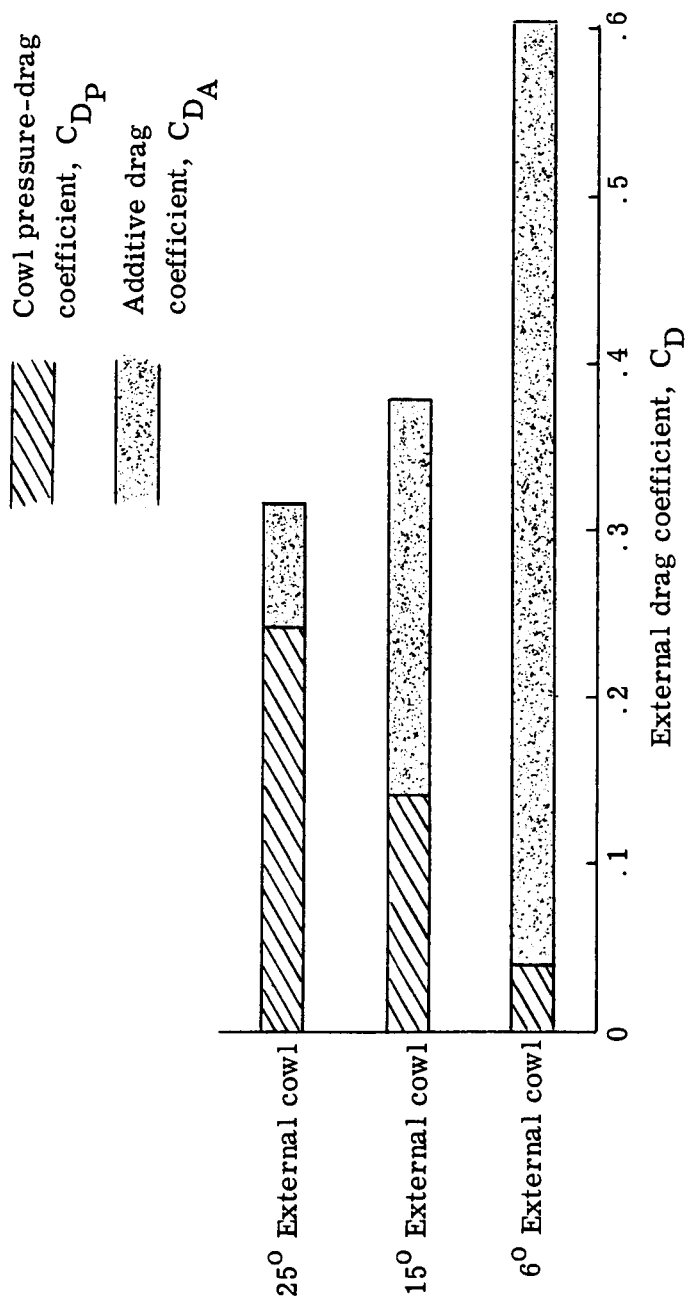
Figure 10. – Comparison of external drag for supercritical inlet operation at Mach 2.49 and angle of attack of 0°.

(a) Configuration A, flush slot bleed.

(b) Configuration B, flush slot bleed.

(c) Configuration C, perforated bleed.

(d) Configuration D, perforated bleed.
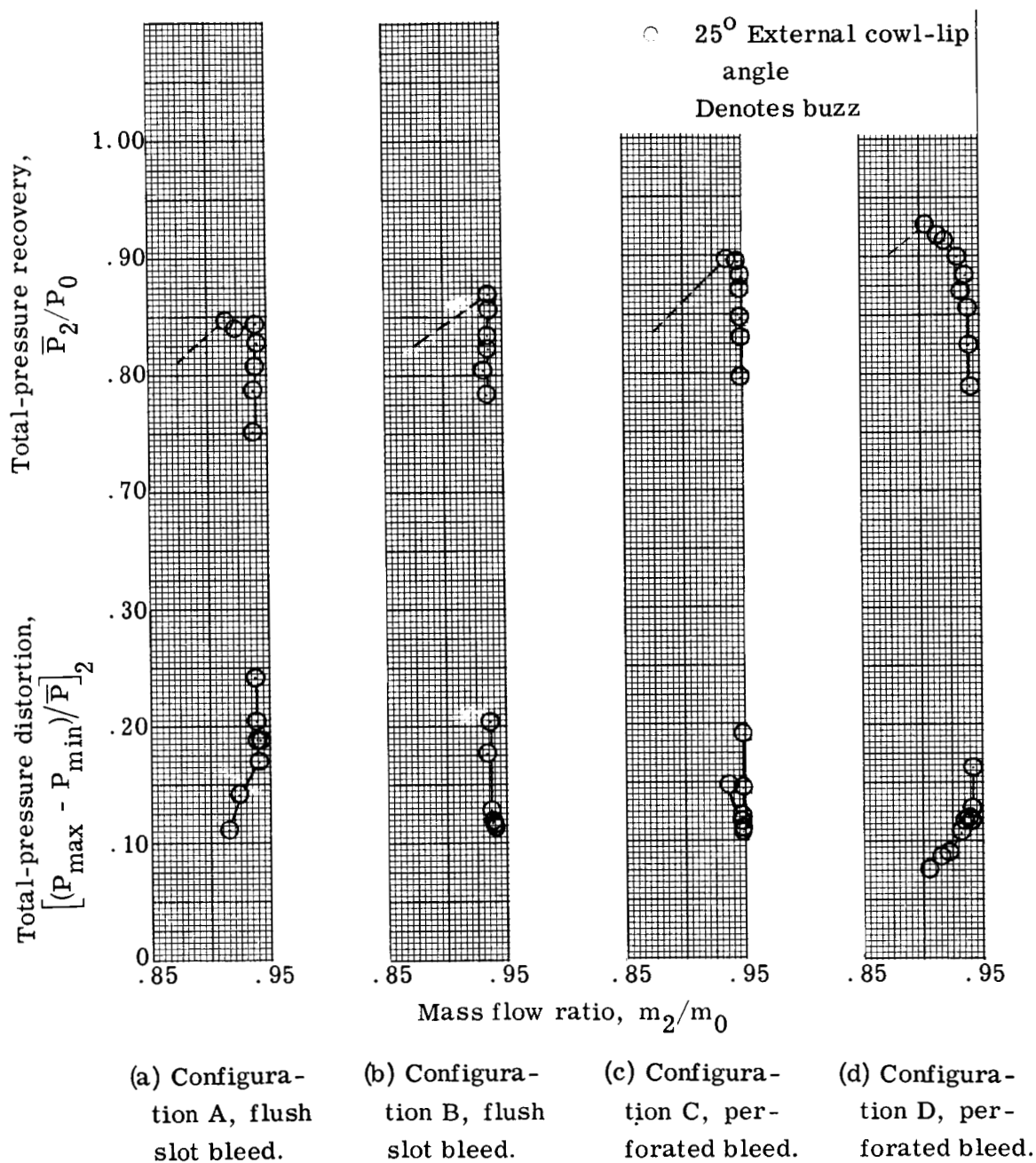
Figure 11. - Effect of spike and bleed modifications on inlet performance at Mach 2.49 and angle of attack of 0°.

(a) Original spike.

C-67-4349
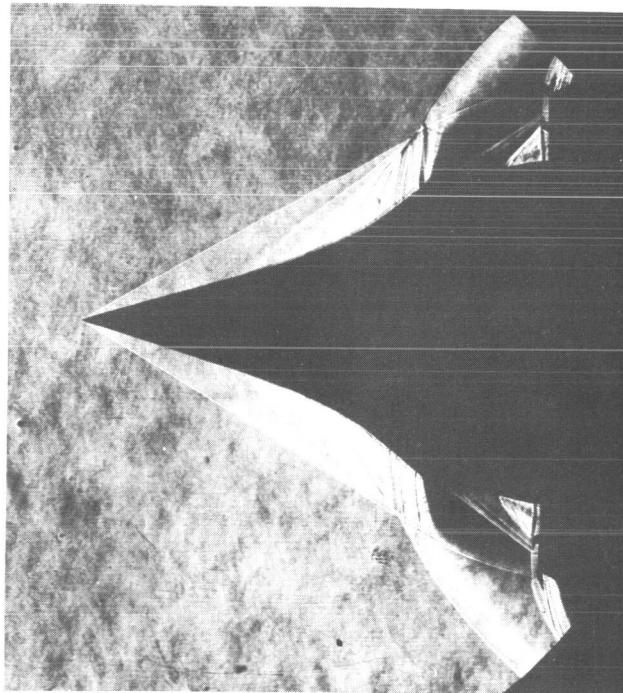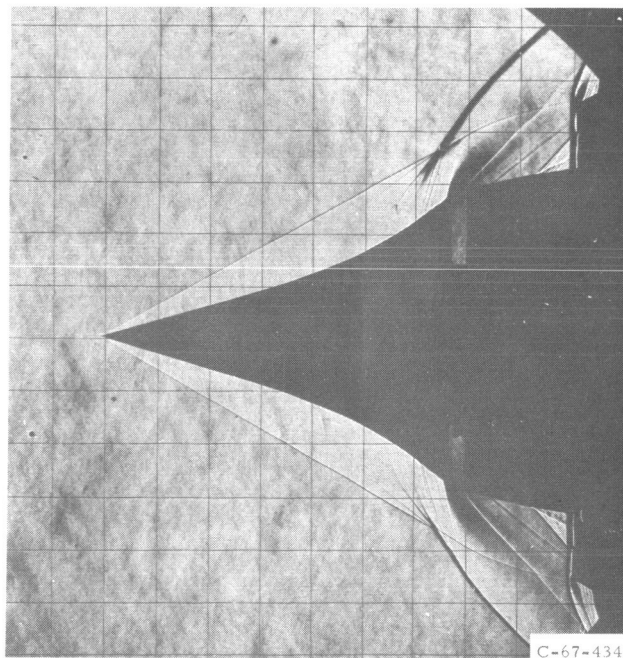
(b) Revised spike.

Figure 12. - Comparison of focusing characteristics of original and revised spike designs at free-stream Mach number of 2.49 and angle of attack of 0°.

Configuration

C, D
B
A

C, D
B
A

A
B
C, D

Angle of attack, α, deg

Critical total-pressure recovery, $\left(\dfrac{\overline{P}_2/P_0}{}\right)_{crit}$

Critical mass flow ratio, $(m_2/m_0)_{crit}$

Critical total-pressure distortion, $\left[(P_{max} - P_{min})/\overline{P}\right]_{crit,\,2}$

Figure 14. – Effect of angle of attack on critical performance at Mach 2.49 for 25° inlet.

C-67-4350

Figure 13. – Schlieren photograph of 25° external cowl-lip angle inlet configuration with revised spike (configuration D) during supercritical operation at free-stream Mach number of 2.49 and angle of attack of 0°.
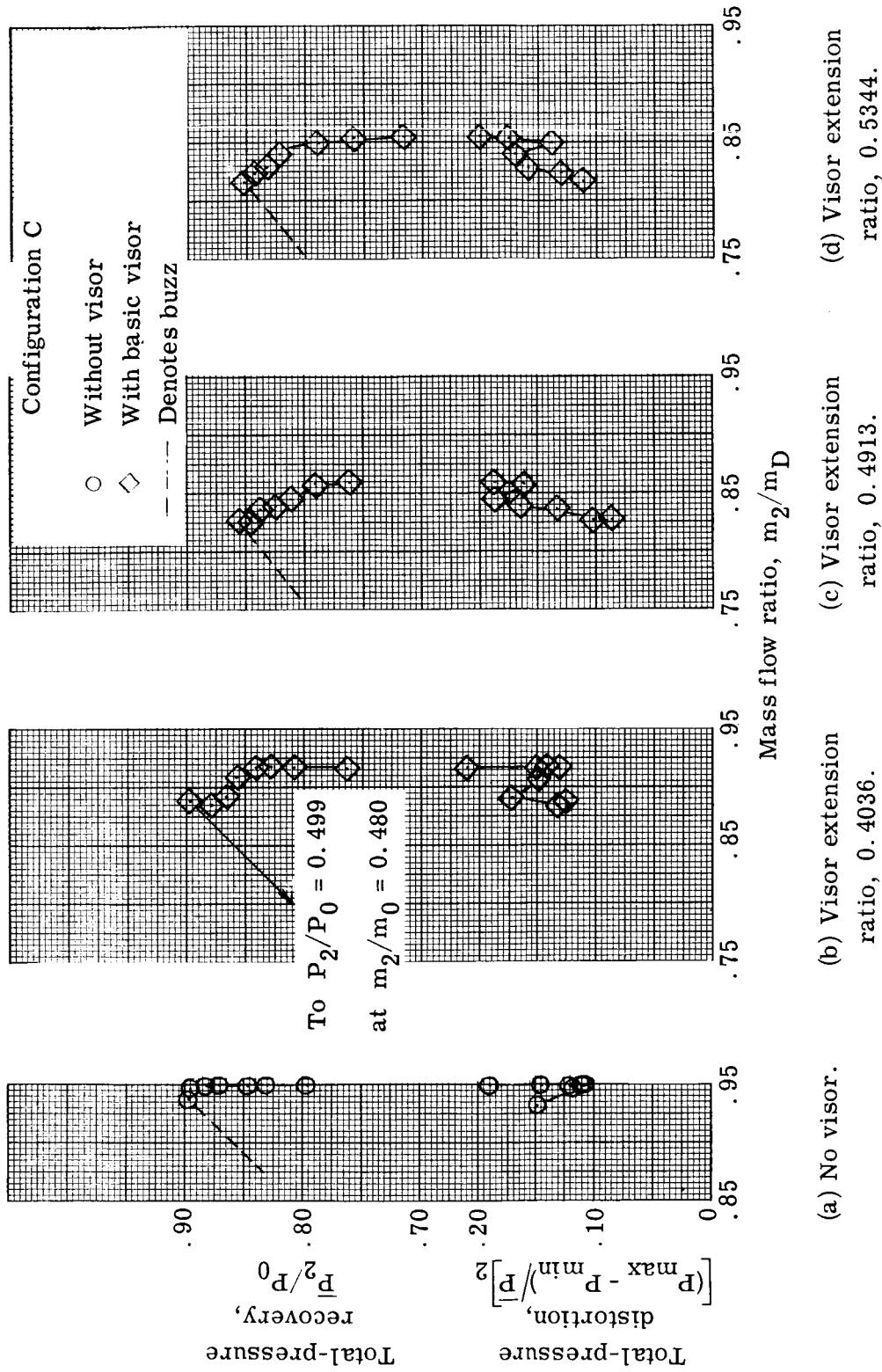
Figure 15. – Effect of cowl visor position on inlet performance at Mach 2.49 and angle of attack of 0°.

C-67-4351
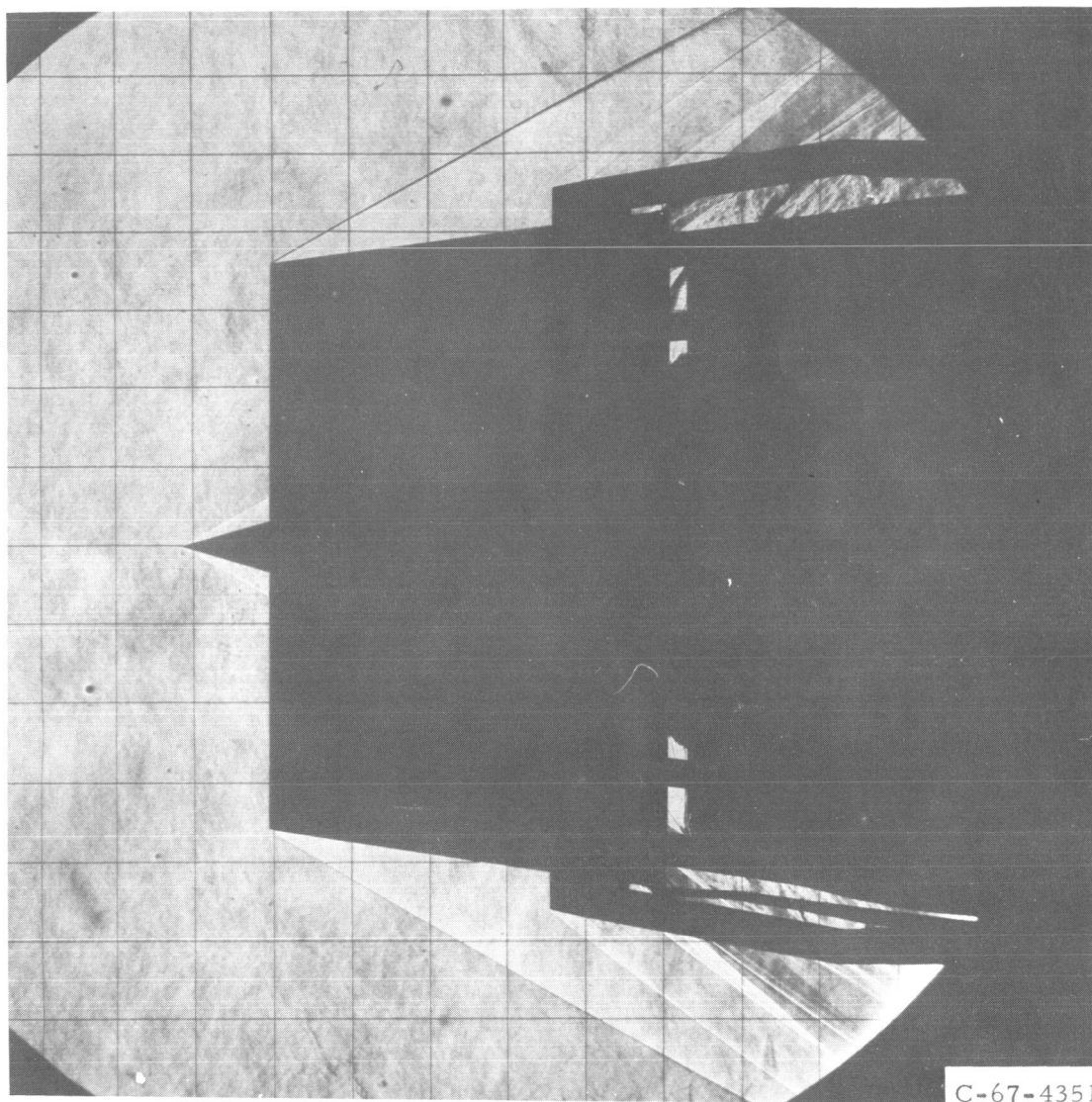
Figure 16. - Schlieren photograph of 25° external cowl inlet (configuration C) with basic visor. Supercritical inlet operation at free-stream Mach number of 2.49, angle of attack of 0°, and visor extension ratio of 0.4913.
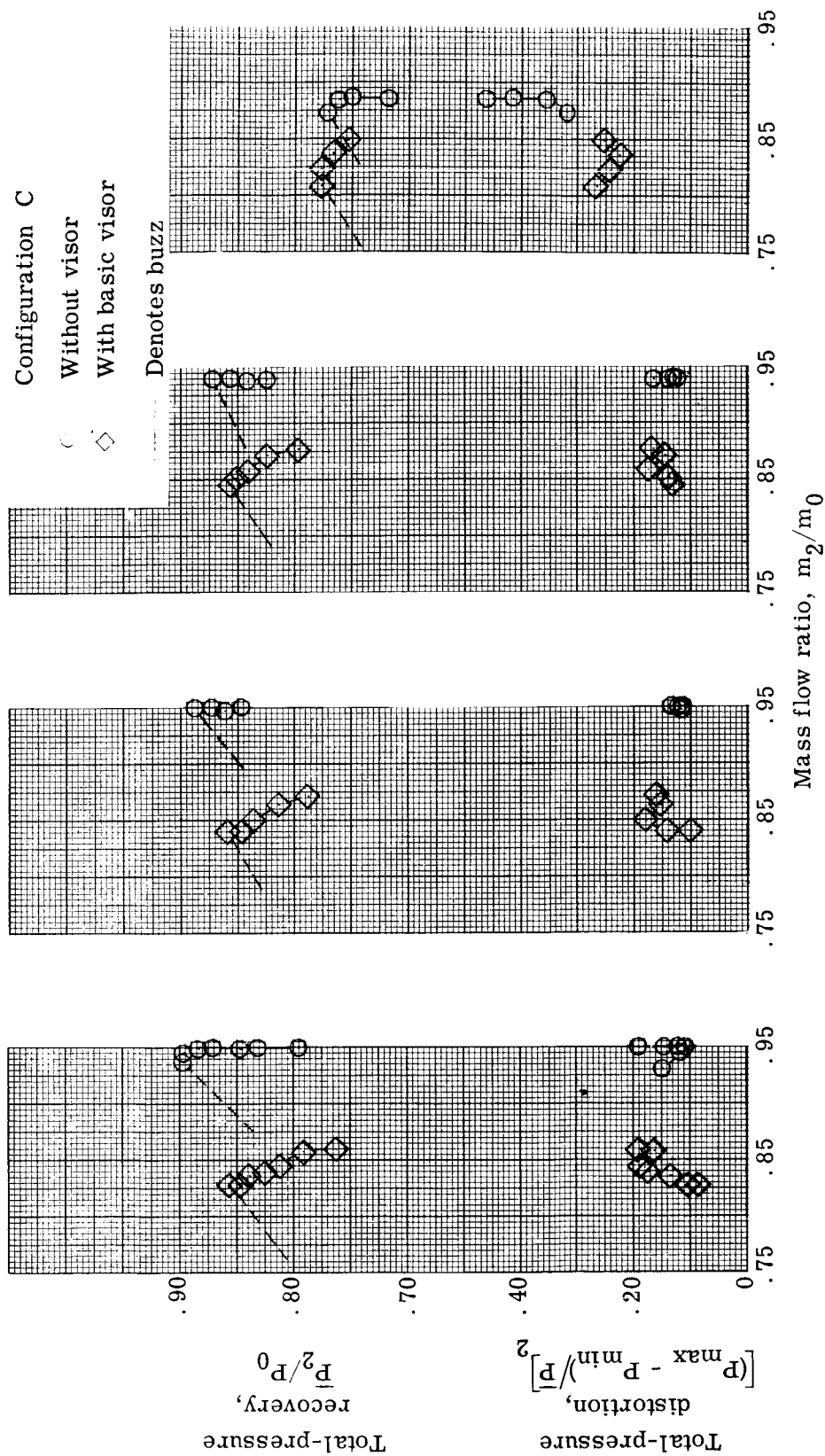
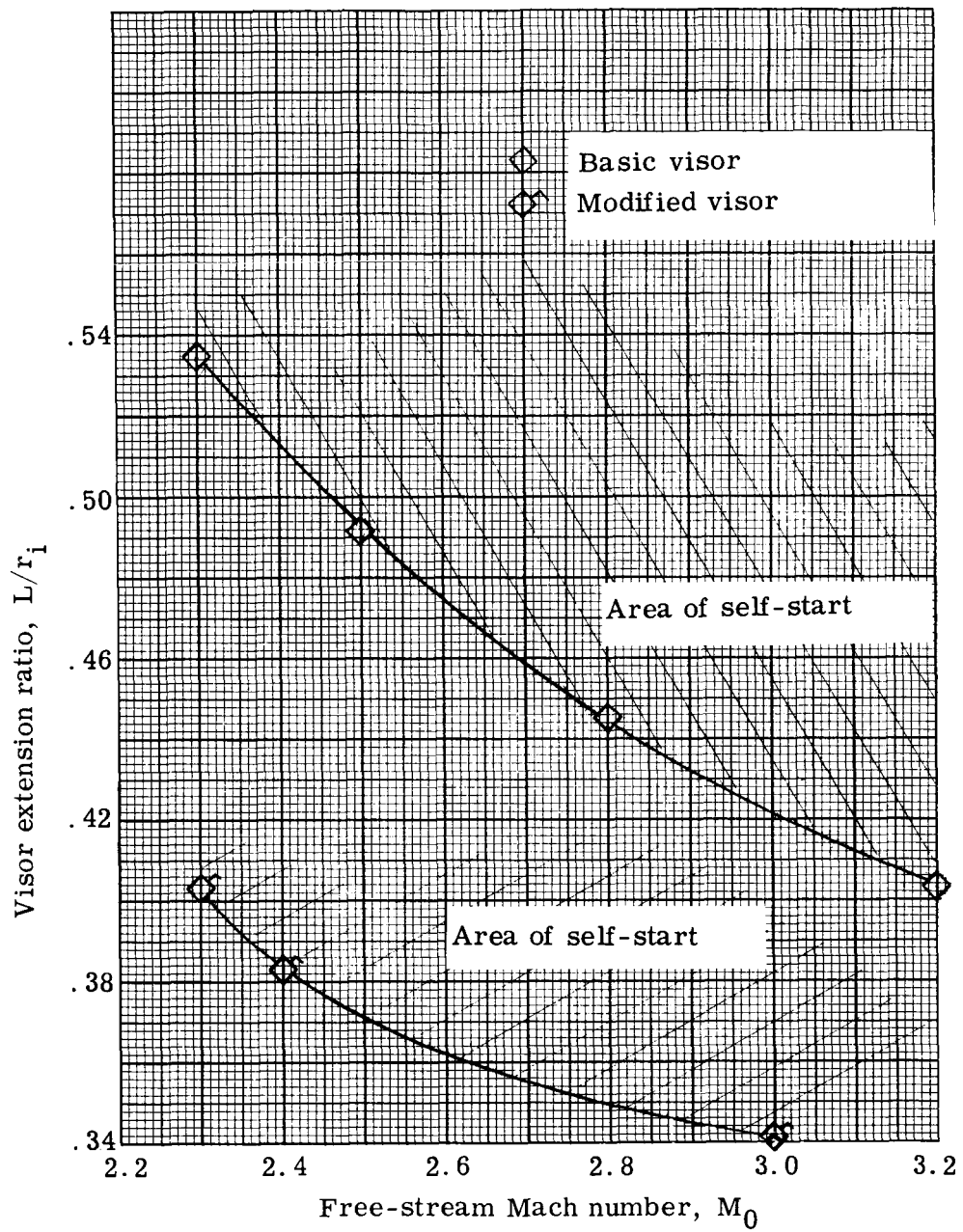Figure 17. - Effect of angle of attack on visored inlet performance at Mach 2.49 and visor extension ratio of 0.4913.

(a) Angle of attack, 0°.   (b) Angle of attack, 1^O.   (c) Angle of attack, 2^O.   (d) Angle of attack, 5°.

Figure 18. - Visor extension required for self-start inlet at 0° angle of attack for various Mach numbers.
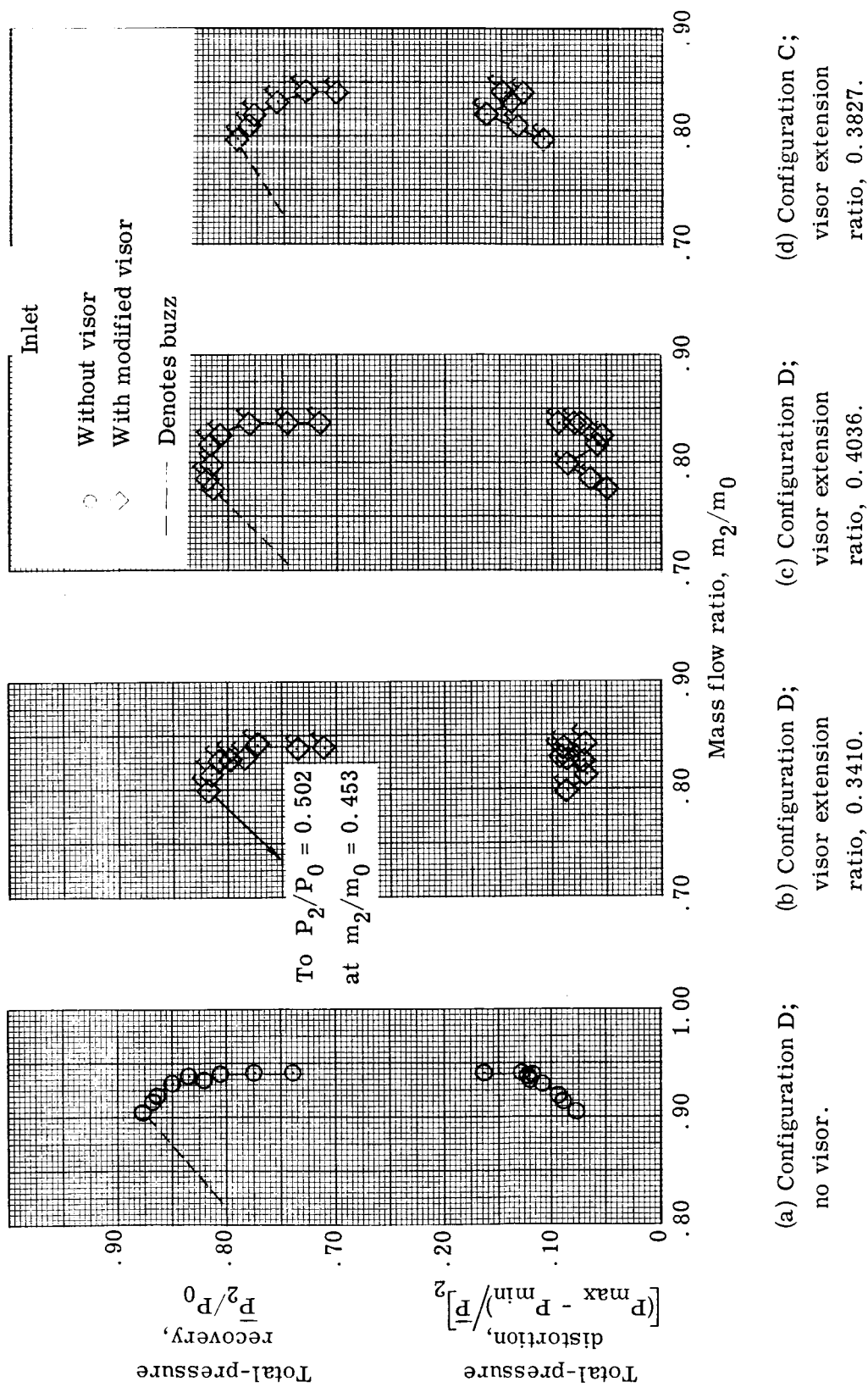
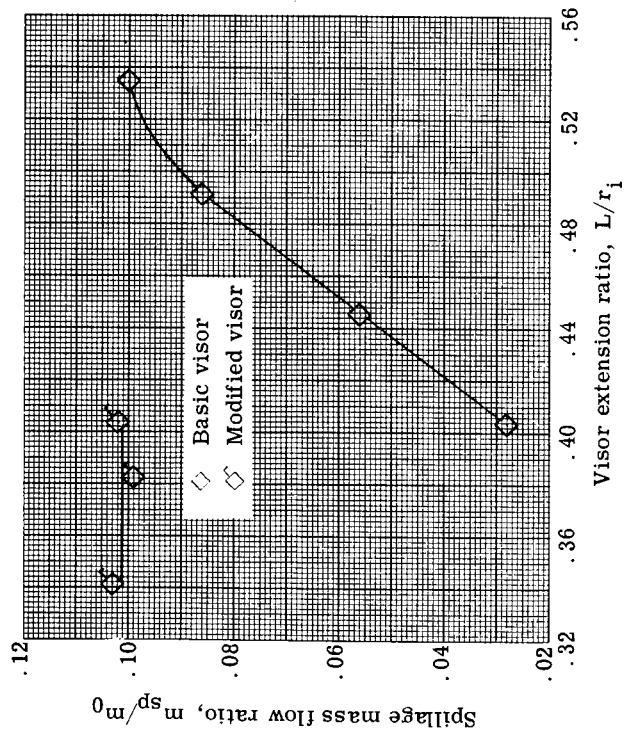Figure 19. - Effect of cowl visor position on inlet performance at Mach 2.49 and angle of attack of 0°.

Figure 21. – Effect of visor position on external drag at Mach 2.49.

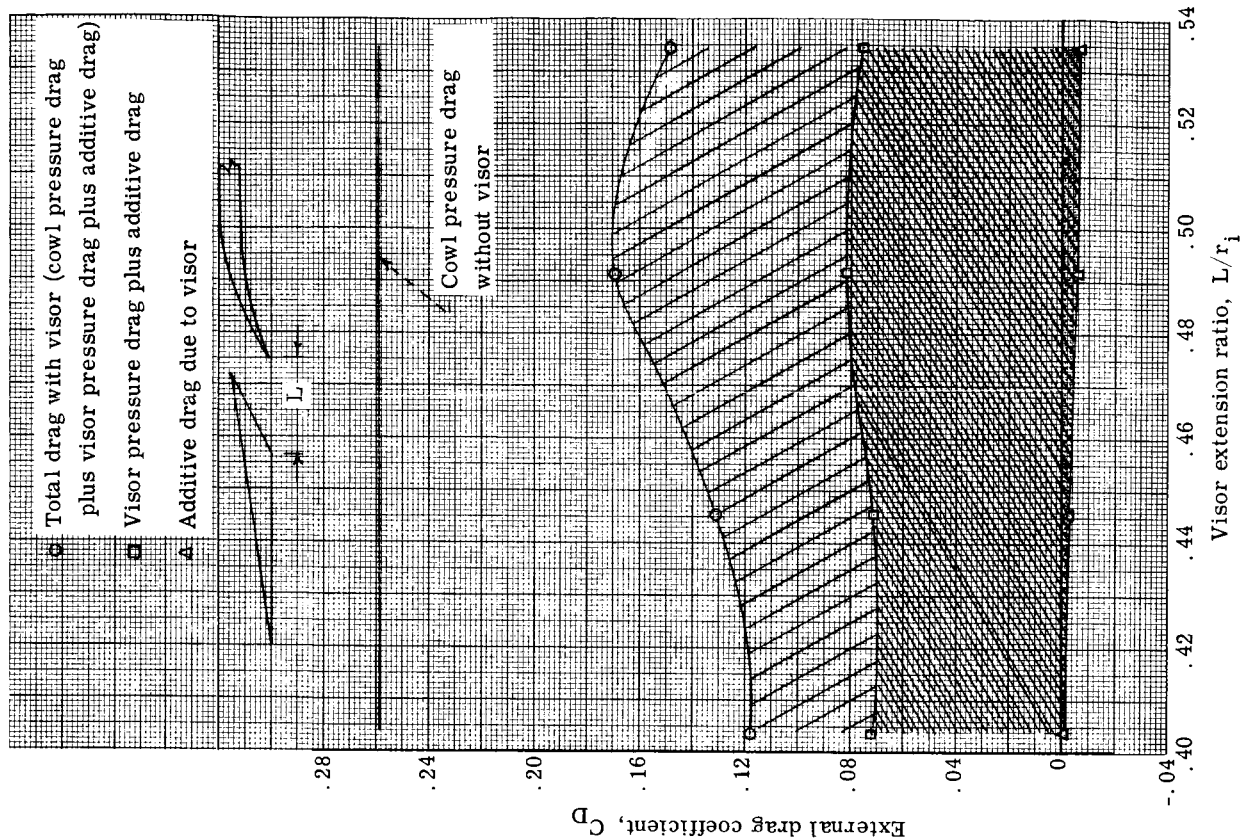Figure 20. – Visor-induced flow spillage for supercritical inlet operation at Mach 2.49 and angle of attack of 0°.

(a) Basic visor.
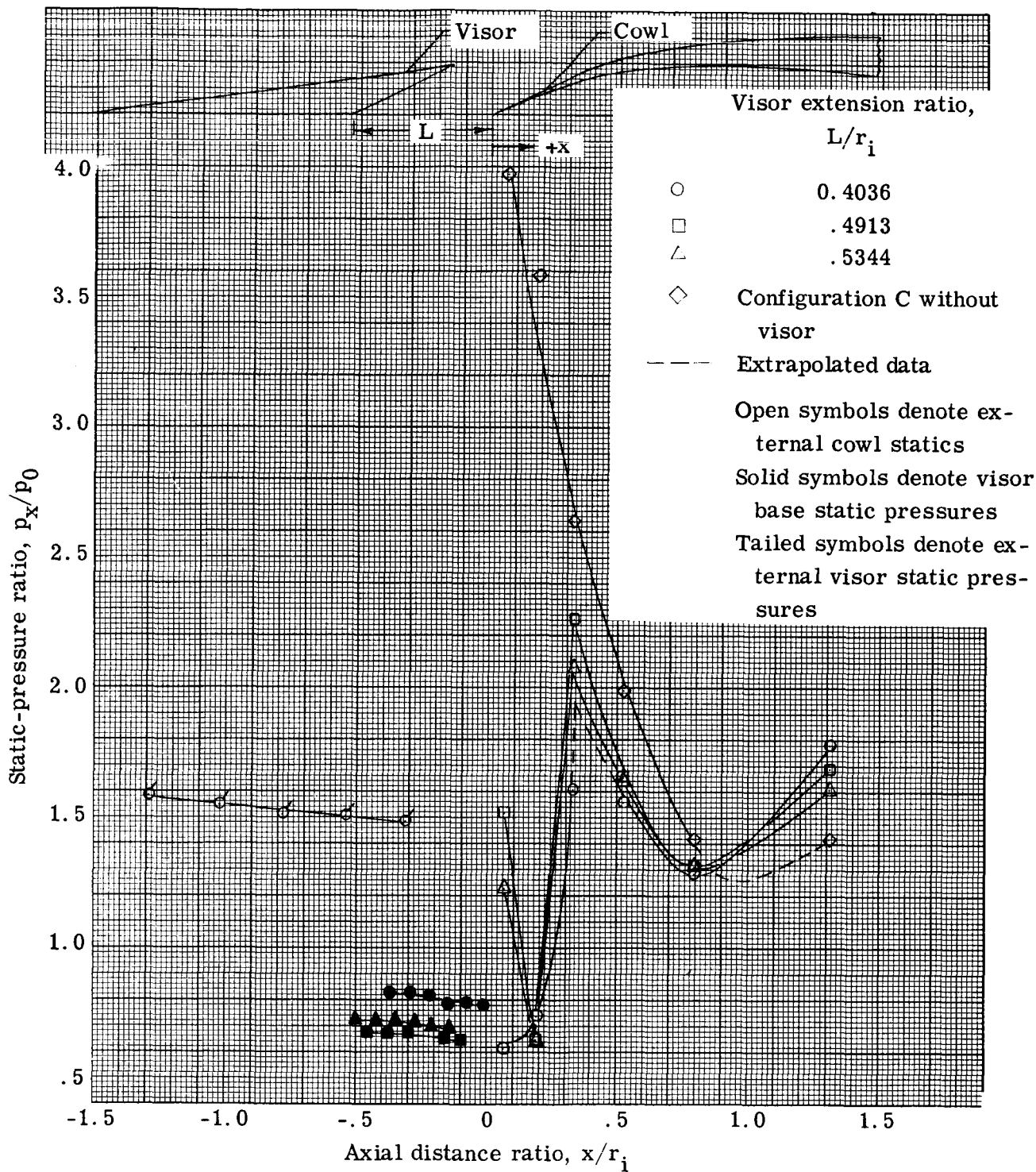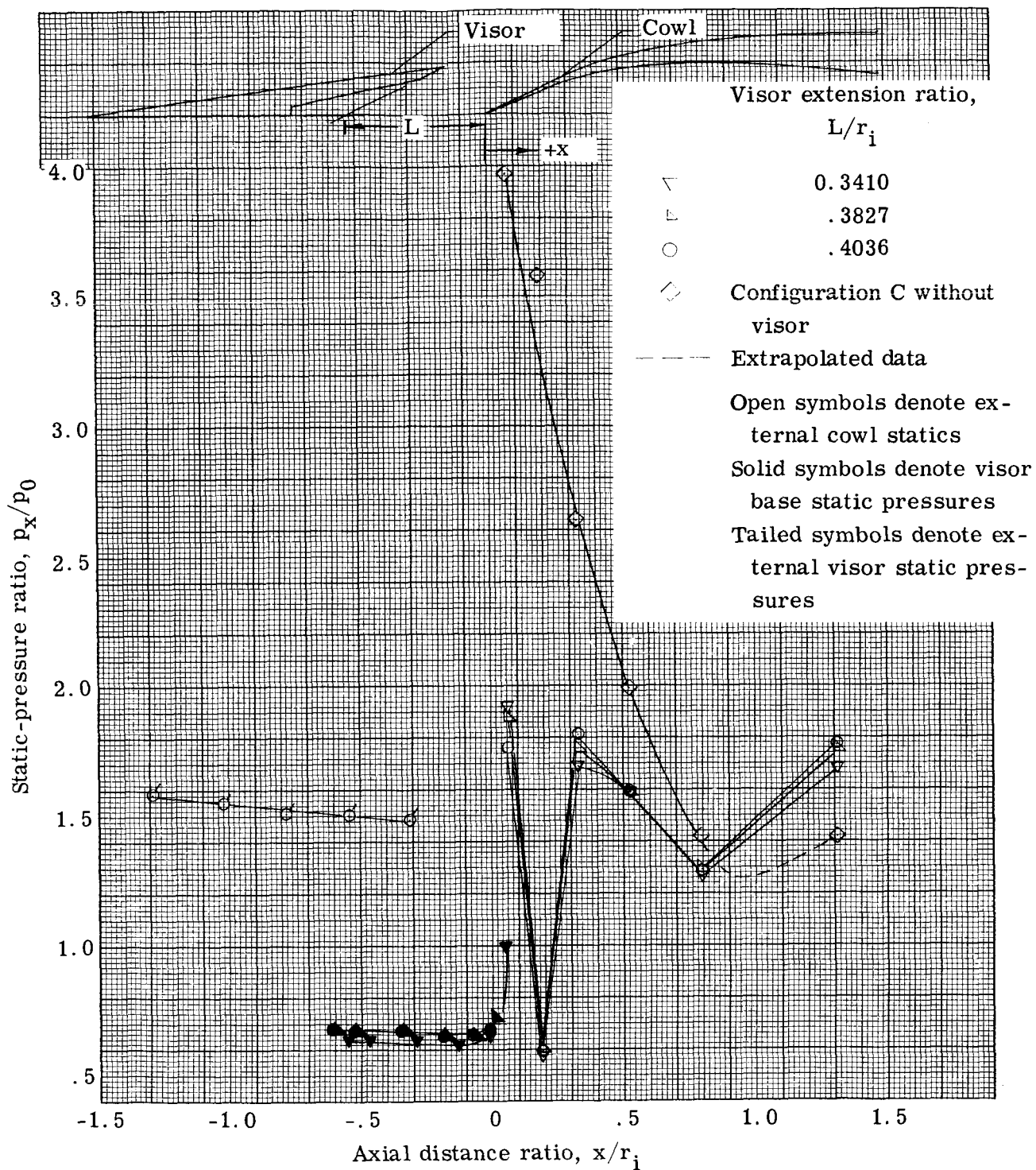
Figure 22. - Static-pressure distributions for supercritical inlet operation at Mach 2.49 and angle of attack of 0°.

(b) Modified visor.

Figure 22. - Concluded.